Applied Energy 250 (2019) 175–184

Contents lists available at ScienceDirect

Applied Energy

journal homepage: www.elsevier.com/locate/apenergy

Peak shaving performance of coal-fired power generating unit integrated with multi-effect distillation seawater desalination

Yuan Xue[a], Zhihua Ge[a,*], Lijun Yang[a], Xiaoze Du[b,*]

[a] Key Laboratory of Condition Monitoring and Control for Power Plant Equipment (North China Electric Power University), Ministry of Education, Beijing 102206, China
[b] School of Energy and Power Engineering, Lanzhou University of Technology, Lanzhou 730050, China

HIGHLIGHTS

- Desalination system is proposed to improve the dispatchability of power plants.
- Peak shaving capacity curve of the water and power co-generation unit is obtained.
- Dynamic response of low-temperature multi-effect distillation system is analyzed.
- Single desalination system has little impact on power generating.
- Proper reduction in motive steam pressure can reduce water production cost.

ARTICLE INFO

Keywords:
Coal-fired thermal power generation
Dispatchability
Dynamic analysis
Multi-effect distillation

ABSTRACT

The peak-load regulation of a coal-fired power plant is critical to promote renewable energy power generation in grid systems. A low-temperature multi-effect distillation (LT-MED) was proposed to improve the dispatchability of a 600 MW coal-fired power generating unit; here, an unsteady thermal system model was established using the Ebsilon software to study peak shaving capacities. The results show that the increased extraction amount and pressure will reduce the power generation and increase the coal consumption. The peak shaving capacity curve was obtained based on the extraction amount. It is indicated that the peak shaving capacity can reach a maximum of 477 MW when the amount of steam extraction is less than 238 ton/h. When the amount of extraction is sufficiently large, the exhaust steam from the low-pressure turbine attains the minimum allowable value, the peak shaving capacity of the unit then sharply decreases. The dynamic response of an LT-MED system to the step variation of the output load of the power generating unit was also revealed. Moreover, the power generation and coal consumption are slightly influenced by the steam consumption in a single LT-MED system. The maximum extraction of the unit can afford a maximum of 19 LT-MED systems. The results of this study will provide a useful reference for the peak shaving of coal-fired power generating units.

1. Introduction

Industrial development depends on energy, however, fossil fuels lead to environmental deterioration. Therefore, the development of clean energy sources, such as wind, solar, and other renewables, has become an inevitable trend. Taking China as an example, it is estimated that by 2020, China's installed wind power capacity will reach 210 million kilowatts, and the installed solar power capacity will reach 110 million kilowatts [1,2].

At present, although the installed capacity of wind and solar power in China has reached 16.54%, the power generation accounted for only 6% at the end of 2017 [3]. This is owing to the random, fluctuating power generation of these renewable energy sources, which has placed significant pressure on the safe operation and supply of power systems [4]. In addition, on the energy demand side, the peak-to-valley difference of the power load in the energy system is increasing, generating further obstacles for the grid to accept renewable energy. Many studies have focused on the prediction of electricity generated by renewable energy sources such as wind [5] and complementary systems of wind and solar [6], and on how to reduce the forecasting uncertainty [7].

Because coal is the major energy resource in China, coal-fired thermal power generation will remain the main form of power generation in China for a long period. Considering the rapidly developing application of renewable energy sources in the grid, it is necessary to

* Corresponding authors.
E-mail addresses: gezh@ncepu.edu.cn (Z. Ge), duxz@ncepu.edu.cn (X. Du).

https://doi.org/10.1016/j.apenergy.2019.04.190
Received 12 February 2019; Received in revised form 28 April 2019; Accepted 30 April 2019
Available online 09 May 2019
0306-2619/

Nomenclature

A_s	Evaporator cross-section area, m^2
BMCR	Boiler maximum continuous rating
BPE	Boiling point elevation, °C
C_p	Specific heat at constant pressure, kJ/(kg·K)
CR	Concentration ratio of seawater
GOR	Gain output ratio
h	Enthalpy, kJ/kg
L	Level, m
LMTD	Logarithmic mean temperature difference, °C
P	Pressure, kPa
PCF	Pressure correction factor
Q	Heat transfer rate, kW
q	Heat flux, W/m^2
R_α	Entrainment ratio
T	Temperature, °C
T_f	Inlet seawater temperature, °C
T_{fin}	Temperature of seawater under first two effects, °C
TCF	Temperature correction factor
THA	Turbine heat acceptance
U	Overall heat transfer coefficient, $kW/(m^2 \cdot K)$
W	Mass flow rate, kg/s
X	Salinity, g/kg

Greek symbols

λ	Latent heat, kJ/kg
ρ	Density, kg/m^3

Subscripts

b	Brine
con	Condenser
d	Distillate
e	Evaporator
ev	Entrained vapor
feed	Feed water
i	Serial number of the evaporator
m	Compressed vapor
o	Outlet
pre	Preheater
s	Steam
v	Secondary vapor
w	Condensate water

improve the dispatchability of coal-fired power generation.

There are generally three types of load peak shaving operation modes for conventional coal-fired power generating units [8]: a two-shift operation, start-stop in turn peak operation, and variable load operation. A two-shift operation refers to the normal operation of the unit during the day and a shut-down when the electrical load is low at night. Under this condition, the load can be considerably adjusted, although such an operation is complicated and requires highly reliable equipment. A start-stop in turn operation means that the units are arranged such that they can start and stop at regular intervals using a regional power grid. However, because of the many factors that require consideration, this method is not widely used. A variable load operation means that when the grid load is low, the power units can run stably under an extremely low load. When the grid load peaks, the unit can operate under a rated or even higher load. This is the most common way to regulate peak loads requiring the power unit to increase and decrease the load quickly and safely.

The dispatchability of the coal-fired thermal power units is mainly affected by the boiler performance, steam turbine performance, and environmental pollution. The minimum load of the boiler usually refers to a stable combustion load without oil. When the boiler load is below this limit, serious safety issues may be caused by the co-combustion of oil and coal. Therefore, the minimum steady-state load of the boiler is also used as the minimum load of the boiler during peak shaving. For boilers designed to use bituminous coal, 30% of the boiler maximum continuous rating (BMCR) is typically set to the minimum steady-state load. However, for safe operation, the plant is usually controlled at 40% or 50% of the rated load [9]. For steam turbines, there is a minimum mass flow rate of the low-pressure cylinder. This is owing to the decrease in the load resulting in a lower inlet mass flow rate of the low-pressure cylinder. When below a certain value, the inlet steam cannot fill the entire flow passage, leading to a backflow, which will form erosion and cause the surface of the low-pressure cylinder blade to be unevenly heated and bent, or even fracture, affecting the safe operation of the turbine [10]. Furthermore, although all existing coal-fired power plants are equipped with desulfurization and denitrification equipment to meet the pollutant discharge standards when a unit is operating at low load, the equipment may not operate normally and cause environmental pollution.

When there is a need to increase the share of renewable energy in the grid, several approaches can be adopted to reduce the load of a coal-fired power plant. This is mainly related to energy storage technologies, including electrical energy storage [11] and thermal storage [12]. However, a large number of studies in this area have been based on simulations and are restricted by immature technologies and the high price of the materials used, and thus have not been applied at a large scale [13]. By contrast, seawater desalination is a mature technology that has been developed for many years and is widely used worldwide.

There has recently been a rapid development in the co-generation of water and power in off-shore thermal power plants. From 2007 to 2015, the capacity of installed seawater desalination plants globally increased from 47.6 Mm^3/d to approximately 97.5 Mm^3/d [14], and is expected to grow to 192 Mm^3/d by 2050 [15]. As one of the main desalination technologies, low-temperature multi-effect distillation (LT-MED) requires approximately 4–7 kWh/m^3 of thermal energy and 1.5–2 kWh/m^3 of electrical energy [16]. Because the top brine temperature of LT-MED is lower than 70 °C, scaling and corrosion are effectively reduced. At the same time, this feature also makes it possible to make full use of various forms of waste heat. At present, studies on the LT-MED system have mainly focused on the following aspects: heat transfer and fouling characteristics in a heat exchanger [17], an overall performance study of the system [18], and integration with different forms of energy, such as waste heat [19], solar energy [20], geothermal energy [21], and nuclear energy [22]. Considering the enormous energy consumption of large-scale seawater desalination plants, thermal seawater desalination systems are often combined with a thermal power plant, which generates a significant amount of waste heat. It has been shown that a combination of water and power generation can improve the thermal efficiency from the present 44% to greater than 60% [23].

The combination of thermal power generation and LT-MED has shown significant potential in both reducing the cost of water production, and increasing the amount of electric power generation and low-grade heat consumption, hence improving the dispatch capability of the thermal power generating units. Applying the surplus power during a low-load period to seawater desalination, thereby converting hard-to-store electricity into easy-to-store fresh water, not only can provide energy for water production and supply fresh water for urban demand, it can also alleviate the peak shaving pressure of a thermal power plant.

In the present study, an LT-MED seawater desalination system is combined with a 600 MW coal-fired power generating unit to achieve a

peak shaving of the power output and improve its dispatchability. The influences of the steam extraction points and extraction amount on the power generation and water production are analyzed using Ebsilon modeling software. Based on the thermodynamic model, the engineering equation solver (EES) is used to analyze the performance of the LT-MED system. The steam parameters obtained from Ebsilon are introduced into the desalination system, and solved by programming the EES. For a change in the extraction point and the amount of steam extraction, the dynamic process of the desalination is analyzed and the peak shaving capability curve of the power plant is acquired.

2. System description and analytical model

In the present water and power cogeneration system, with and without consumption of the steam extracted from the turbine and the electric power by the LT-MED system, the output power of the objective generating unit will be adjusted to a significant extent, indicating an improvement in the dispatchability of the present coal-fired power generating unit. In addition, to improve the gained output ratio (GOR) of an LT-MED system, the thermal vapor compressor (TVC) was introduced into the desalination system. Fig. 1 shows a photograph of a practical water and power cogeneration system.

Fig. 2 shows a schematic diagram of the thermo-flow processes of both a power generating unit and a TVC-LT-MED system, of which the thermodynamic model of the power generating unit was established using Ebsilon software.

As shown in Fig. 2, there are many evaporators used in a desalination system, and are encapsulated during the practical production process, namely, the white body shown in Fig. 1. The steam extracted from the turbine flow through the piping to the desalination system is used as motive steam.

As shown in Fig. 2, the fourth extraction steam of the turbine is used as a heat source of the LT-MED system. The freshwater production of the proposed LT-MED system is set to 12,000 tons/d, corresponding to 50 tons/h of steam extraction of the turbine. There are two steam turbines and two desalination units applied. Practical water production, which depends on the extracted steam, can be provided by the power generating unit during its peak shaving operation.

The physical model of the parallel/cross flow adopted for the LT-MED system in the present study is shown in Fig. 2. The seawater in the condenser is used to cool the secondary steam generated in the final effect. The heat released through condensation of the steam is significant, thereby requiring a large amount of seawater. The seawater in each effect will be heated and then evaporated. Thus, if all seawater enters the effects, it means that more heat is consumed through the heating process than through the evaporation process. Thus, a sufficient amount of secondary steam, which also means freshwater, cannot be produced. Therefore, a portion of the seawater flowing out of the condenser needs to be discharged back into the environment, and the rest divided into two parts. One part enters the 3rd through 6th effects. The other enters the preheater and is heated by the condensed water from the first effect again, and then flows into the first and second effects as a feed seawater. The feed seawater entering the first effect is heated and produces a portion of secondary steam, and the remaining brine flows into the next effect. The pressure and temperature decrease in the direction of the vapor flow, and thus the brine from the former effect that flows into the next effect will flash. The secondary steam generated in the first effect will be condensed after the heating of seawater in the second effect. Condensed water flows into a flash tank to produce more steam in the third effect. The above process is repeated until the last effect [24,25]. The steam extracted from the turbine is used as the heat source of the first effect. The steam from the steam turbine is usually high in terms of pressure and temperature, and can eject the low-pressure secondary vapor from the MED system through the TVC component; thus, the heat can be fully utilized to obtain more steam entering the first effect with a temperature of approximately 65 °C.

The analytical models, including thermodynamic, transient, and steady-state analyses, were established to reveal the dynamic characteristics of the power and water cogeneration system and investigate its peak shaving performances according to the following assumptions.

(1) The difference in terminal temperature of the regenerative heaters shown in Fig. 2(a) remains unchanged.
(2) The temperature of the water circulated into the condenser is set to 20 °C.
(3) The steam consumption of the small steam turbine shown in Fig. 2(a) varies with the main steam quantity, which is consistent with the original system.
(4) The leakage steam parameters of the steam turbine vary with the generation load.

2.1. Thermodynamic analysis

The process modeling of desalination is based on the material, salt, and energy balance equations. To reveal the transient behaviors of the thermal system under a variable power output of the objective generating unit, the unsteady equations can be obtained through their differentiation, as listed in Table 1. The corresponding thermodynamic properties are listed in Table 2.

The mass, energy, and salt balances of the evaporators are expressed as Eqs. (1)–(6) listed in Table 1. For the first effect, there is no prior brine flow into the effect, and hence $W_{b,0} = 0$.

3. Results and analysis

3.1. System simulation and verification

The commercial software Ebsilon was applied to obtain the heat from the boiler and the electric power output of the present coal-fired thermal power generating unit. Ebsilon is widely used in the design, evaluation, and optimization of all power plant types and other thermodynamic processes [29,30]. The main simulation formula of the steam turbine component is the Flugel formula. The simulation results of the power generation are compared with the corresponding reference data, as shown in Table 3. The simulation results of the reference power plant are consistent with the actual data from a power plant with little deviation. Such deviation is mainly caused by uncertainty in the turbine leakage parameters. The simulation results show that the established model is feasible and reliable in simulating the extraction process of a power plant.

Fig. 1. Practical 600 MW coal-fired power generating unit combined with TVC-LT-MED.

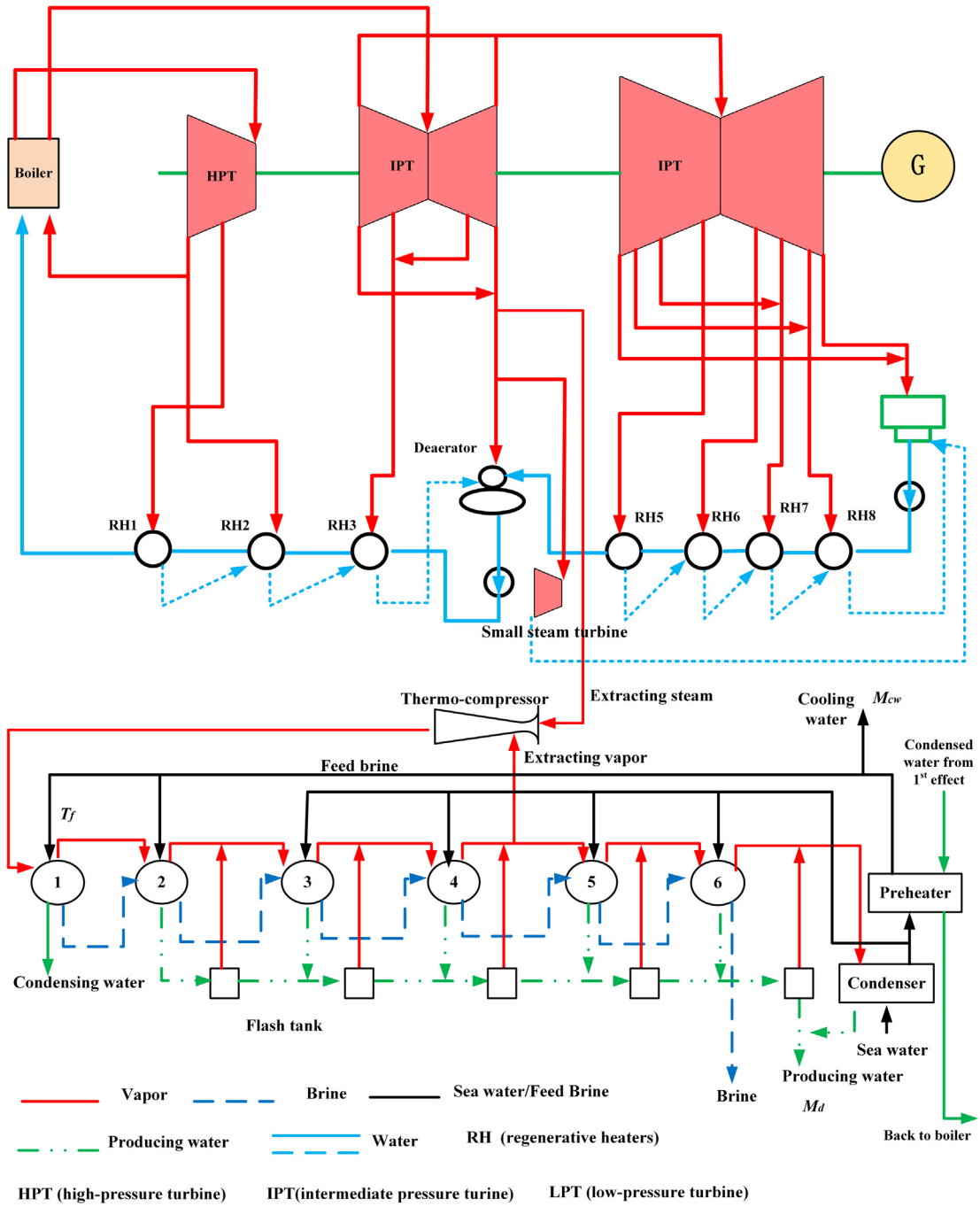

Fig. 2. Schematic of coal-fired power generating unit combined with TVC-LT-MED system.

3.2. Thermodynamic analysis of different extraction points

The steam extracted from the steam turbine is used as a heat source of the LT-MED system in the first effect, and serves as high-pressure steam compressing a portion of the low-pressure steam from the LT-MED system through the TVC. Different steam extraction points and extraction amounts will affect the extraction pressure, which will not only affect the power generation of the objective unit, but also the steam pressure entering the TVC. Therefore, the performance of the LT-MED system will be affected.

Fig. 3 shows the effect of the change in the extraction amount on the power generation and coal consumption of the power generating unit when the extraction point is changed from the third to the sixth stage (indicated as 3C to 6C in Figs. 3 and 4); here, the rate of the main steam flow is equal to that under the THA working conditions.

It can be seen from Fig. 3 that, as the amount of steam extraction increases, the amount of power generation decreases and the coal consumption increases. When the extraction amount is the same, the backward movement of the extraction point leads to an increase in the power generation and the decrease in coal consumption. This is because the closer the extraction point is to the exhaust of the low-pressure cylinder, the lower the pressure and temperature of the steam, and the less energy that is available for the power generation. The increase in the extraction amount reduces the amount of steam flowing out of the turbine, thereby reducing the amount of power generation. In addition, because the main steam mass flow rate is constant, the coal consumption rate increases.

In addition, the extraction amounts of 24.5, 50, and 60 ton/h

Table 1
Modeling of the mass and energy equilibrium of the desalination system [26,27].

Parameters	Formulas	
Mass balance in evaporator	$k_1\frac{dL_i}{dt} + k_2\frac{dT_i}{dt} + k_3\frac{dX_i}{dt} = k_4$	(1)
	$k_1 = A_s\rho_{b,i} - A_s\rho_{v,i}$	(2)
	$k_2 = A_sL_i\frac{\partial\rho_{b,i}}{\partial T_{b,i}}\left[1 + \frac{\partial BPE_i}{\partial T_i}\right] + A_sL_{v,i}\frac{\partial\rho_{v,i}}{\partial T_i}$	
	$k_3 = A_sL_i\left(\frac{\partial\rho_{b,i}}{\partial T_{b,i}}\frac{\partial BPE_i}{\partial X_i} + \frac{\partial\rho_{b,i}}{\partial X_i}\right)$	
	$k_4 = W_{feed} + W_{b,i-1} - W_{b,i} - W_{v,i}$	
Energy balance in evaporator	$k_5\frac{dL_i}{dt} + k_6\frac{dT_i}{dt} + k_7\frac{dX_i}{dt} = k_8$	(3)
	$k_5 = A_s\rho_{b,i}h_{b,i} - A_s\rho_{v,i}h_{v,i}$	(4)
	$k_6 = A_sL_ih_{b,i}\frac{\partial\rho_{b,i}}{\partial T_{b,i}}\left[1 + \frac{\partial BPE_i}{\partial T_i}\right] + A_sL_{v,i}h_{v,i}\frac{\partial\rho_{v,i}}{\partial T_i}$	
	$+ A_sL_i\rho_{b,i}\frac{\partial h_{b,i}}{\partial T_{b,i}}\left[1 + \frac{\partial BPE_i}{\partial T_i}\right] + A_sL_{v,i}\rho_{v,i}\frac{\partial h_{v,i}}{\partial T_i}$	
	$k_7 = A_sL_ih_{b,i}\left(\frac{\partial\rho_{b,i}}{\partial T_{b,i}}\frac{\partial BPE_i}{\partial X_i} + \frac{\partial\rho_{b,i}}{\partial X_i}\right) + A_sL_i\rho_{b,i}\left(\frac{\partial h_{b,i}}{\partial T_{b,i}}\frac{\partial BPE_i}{\partial X_i} + \frac{\partial h_{b,i}}{\partial X_i}\right)$	
	$k_8 = W_{feed}h_{feed} + W_{b,i-1}h_{b,i-1} - W_{b,i}h_{b,i} - W_{v,i}h_{v,i} + Q_{e,i}$	
Salt balance in evaporator	$k_9\frac{dL_i}{dt} + k_{10}\frac{dT_i}{dt} + k_{11}\frac{dX_i}{dt} = k_{12}$	(5)
	$k_9 = A_s\rho_{b,i}X_i$	(6)
	$k_{10} = A_sL_iX_i\frac{\partial\rho_{b,i}}{\partial T_{b,i}}\left[1 + \frac{\partial BPE_i}{\partial T_i}\right]$	
	$k_{11} = A_sL_i\left(X_i\frac{\partial\rho_{b,i}}{\partial T_{b,i}}\frac{\partial BPE_i}{\partial X_i} + X_i\frac{\partial\rho_{b,i}}{\partial X_i} + \rho_{b,i}\right)$	
	$k_{12} = W_{feed}X_{feed} + W_{b,i-1}X_{b,i-1} - W_{b,i}X_{b,i}$	
Heat transfer rate of evaporator	$Q_{e,i} = U_{e,i}A_{e,i}(T_{v,i-1} - T_{v,i})$	(7)
Energy balance in condenser	$V_{con}\rho_{con}\frac{dh_{con}}{dt} = Q_{con} - W_{con}C_p(T_{feed} - T_f)$	(8)
	$Q_{con} = U_{con}A_{con}LMTD_{con}$	
Energy balance in preheater	$V_{pre}\rho_{pre}\frac{dh_{pre}}{dt} = Q_{pre} - W_{pre}C_p(T_{fin} - T_{feed})$	(9)
	$Q_{pre} = U_{pre}A_{pre}LMTD_{pre}$	
Brine flow rate	$W_{b,i} = C_{b,i}\sqrt{\Delta P_{b,i}}$	(10)
	$\Delta P_{b,i} = P_{i-1} - P_i + \rho_b g(L_{i-1} - L_i)$	
Vapor flow rate	$W_{v,i} = \frac{W_{v,i-1}L_{i-1} - W_{feed}C_p(T_i - T_{feed}) + W_{b,i-1}C_{pb}(T_{i-1} - T_i)}{L_i}$	(11)
Overall material balance of ejector	$W_s = W_m + W_{ev}$	(12)
Entrainment ratio	$R_\alpha = W_m/W_{ev}$	(13)
	$R_\alpha = 0.296\frac{(P_s)^{1.19}}{(P_{ev})^{1.04}}\left(\frac{P_m}{P_{ev}}\right)^{0.015}\left(\frac{PCF}{TCF}\right)$	(14)
	$PCF = 3 \times 10^{-7}(P_m)^2 - 0.0009P_m + 1.6101$	(15)
	$TCF = 2 \times 10^{-8}(T_{ev})^2 - 0.0006T_{ev} + 1.0047$	(16)
Performance analysis	$GOR = \frac{W_d}{W_{steam}}$	(17)
Concentration ratio of seawater	$CR = \frac{X_{b(n)}}{X_{f(1)}}$	(18)

correspond to the 40%, 100%, and 110% operating conditions of the LT-MED system investigated in the present study, respectively. Taking into account the original two desalination plants with a production amount of 10,000 ton/d, a steam extraction of 50 tons/h per equipment, and two steam turbines, the above three working conditions of the LT-MED correspond to the 62.5, 75, and 80 ton/h extracted from the turbine, respectively, as shown in Fig. 3.

Fig. 4 demonstrates the fresh water production and gain output ratio (GOR) of the new desalination system under 40%, 100%, and 110% operation conditions under different extraction points. The three mass flows in the legend correspond to the three operating conditions. It can be seen from Fig. 4 that the backward movement of the extraction point causes fresh water production to decrease with the same extraction amount, which is consistent with the trend of the GOR. The backward movement of the extraction point means that the extracted steam pressure is reduced. The high-temperature and high-pressure steam extract low-pressure steam through the TVC and then enter the first effect. Referring to Eqs. (12)–(16), the low-pressure steam is derived from the fourth effect. The lowering of the extracted steam pressure results in less compressed low-pressure steam, and less steam therefore enters the first effect, thereby reducing the amount of water produced. Similarly, at the same extraction point, a reduction in the extraction amount will also cause the steam entering the first effect to decrease, and the water production will also decrease, as shown in Fig. 4.

3.3. Dynamic response of LT-MED system to the variation in output load of power generating unit

When the water and power cogeneration unit is operated in peak shaving mode, the mass flow rate and pressure of the extraction steam may change at any time, and thus it is necessary to understand the impact of this sudden change on the desalination system. It is assumed that the amount of steam extracted from the steam turbine for seawater desalination suddenly increases from 50 to 60 ton/h after 20 s, and the steam pressure decreases from 750 to 287 kPa at 80 s.

With the initial operating conditions listed in Table 4, the corresponding transient performances of the LT-MED system, including the dynamic curves of the mass flow rate of the secondary vapor, brine level, salinity, and temperature under all effects, are as shown in Fig. 5. For each effect, the seawater is sprayed from the top, and there is a

Table 2
Thermodynamic properties of the desalination system [27,28].

Parameters	Formulas	
Seawater density	$\rho_b = (A_1F_1 + A_2F_2 + A_3F_3 + A_4F_4) \times 10^3$	(19)
	$A_1 = -4.032219 \times 0.5 + 0.115313B + 3.26 \times 10^{-4}(2B^2 - 1)$	
	$A_2 = -0.108199 \times 0.5 + 1.571 \times 10^{-3}B - 4.23 \times 10^{-4}(2B^2 - 1)$	
	$A_3 = -0.012247 \times 0.5 + 1.74 \times 10^{-3}B - 9 \times 10^{-6}(2B^2 - 1)$	
	$A_4 = 6.92 \times 10^{-4} \times 0.5 - 8.7 \times 10^{-5}B - 5.3 \times 10^{-5}(2B^2 - 1)$	
	$B = (2X - 150)/150$	
	$F_1 = 0.5$	
	$F_2 = A$	
	$F_3 = 2A^2 - 1$	
	$F_4 = 4A^3 - 3A$	
	$A = (2T - 200)/160$	
Vapor density	$\rho_v = 0.005059 + 0.00023748T_v + 1.777 \times 10^{-5}T_v^2 - 4.327 \times 10^{-8}T_v^3 + 4.342 \times 10^{-9}T_v^4$	(20)
Boiling point elevation	$BPE = AX + BX^2 + CX^3$	(21)
	$A = (8.325 \times 10^{-2} + 1.883 \times 10^{-4}T + 4.02 \times 10^{-6}T^2)$	
	$B = (-7.625 \times 10^{-4} + 9.02 \times 10^{-5}T - 5.2 \times 10^{-7}T^2)$	
	$C = (1.522 \times 10^{-4} - 3 \times 10^{-6}T - 3 \times 10^{-8}T^2)$	
Seawater enthalpy	$h_b = (h_w - X/1000\cdot(-2.34825 \times 10^4 + 315.183X + 2.80269X^2 - 0.0144606X^3 + 7826.07T_b - 44.1733T_b^2 + 0.21394T_b^3 - 19.9108XT_b + 0.0277846X^2T_b + 0.0972801XT_b^2)) \times 10^{-3}$	(22)
Vapor enthalpy	$h_v = 2501.689845 + 1.806916015T_v + 5.087717 \times 10^{-4}T_v^2 - 1.221 \times 10^{-5}T_v^3$	(23)
Heat transfer coefficient of evaporator	$U_e = (1939.4 + 1.40562T - 0.0207525T^2 + 0.0023186T^3) \times 10^{-3}$	(24)
Heat transfer coefficient of condenser	$U_{con} = (1617.5 + 0.1537T_{con} + 0.1825T_{con}^2 - 0.00008026T_{con}^3) \times 10^{-3}$	(25)
	$T_{con} = (T_{feed} + T_f)/2$	
Latent heat of vaporization	$\lambda = 2501.897149 - 2.407064037T_v + 1.192217 \times 10^{-3}T_v^2 - 1.5863 \times 10^{-5}T_v^3$	(26)
Specific heat of seawater	$C_p = 10^{-3} \times (A + BT + CT^2 + DT^3)$	(27)
	$A = 4206.8 - 6.6197X + 1.2288 \times 10^{-2}X^2$	
	$B = -1.1262 + 5.4178 \times 10^{-2}X - 2.2719 \times 10^{-4}X^2$	
	$C = 1.2026 \times 10^{-2} - 5.3566 \times 10^{-4}X + 1.8906 \times 10^{-6}X^2$	
	$D = 6.8777 \times 10^{-7} + 1.517 \times 10^{-6}X - 4.4268 \times 10^{-9}X^2$	

Table 3
Comparison of the simulated results and the actual data of the objective power generating unit shown in Fig. 1.

Conditions	Simulated results (MW)	Reference values (MW)	Deviation (%)
VWO	661.472	661.996	−0.07922
100% THA	600.229	600.405	−0.02928
75% THA	451.73	450.179	0.34461
50% THA	302.488	300.8	0.80245
40% THA	242.728	240.083	1.10173
30% THA	184.247	180.127	2.28748

certain amount of non-vaporized seawater at the bottom of the evaporator. The height of this part of the seawater is at the brine level.

When the amount of seawater in each effect remains unchanged, the increase in steam flow means an increase in the amount of heat exchange, as shown in Fig. 5(a). At 20 s, the secondary steam flow in each effect suddenly increases. The decrease in steam pressure means that the steam enthalpy decreases and the heat exchange rate decreases, and thus at 80 s, the curve of secondary steam at each effect decreases. As can be seen in Fig. 5(b), the effects of the steam amount and pressure changes on the brine level are small and are most evident in the first effect. The curve decreases at 20 s and increases at 80 s. This change is consistent with the analysis in Fig. 5(a), and as the number of effects increases, the amount of concentrated brine flowing into the subsequent effect gradually increases; thus, the change becomes gradually less clear.

Fig. 5(c) shows the variations in salinity for each effect. According to the analysis in Fig. 5(a), at 20 s, the secondary steam generated at each effect increases, resulting in a decrease in the concentrated brine. Thus, according to the salt balance, the increase in steam flow causes an increase in the salinity of the seawater. As shown in Fig. 5(d), the sudden increase in the steam flow causes a decrease in temperature for each effect, and the reduction of the latter effect is greater than that of the previous effect. The reason behind this behavior is that, based on the feed flow rate, the brine flows from the previous effect, and the temperature of the previous effect will affect the temperature of each effect owing to a delay. At 80 s, the decrease in steam pressure causes the temperature of each effect to increase.

3.4. Thermodynamic analysis of extraction amount under design and off-design conditions

Section 3.2 provides only an analysis for when the main steam is equal to the THA condition. To clarify the influence of the steam consumption of the LT-MED system on the power plant, the effects of the extraction amount corresponding to different LT-MED operating conditions on the performance of a power plant under both the design and off-design conditions are analyzed as follows.

Considering that the top brine temperature of the LT-MED is lower than 70 °C, if the extraction pressure of steam from the turbine is too high, a waste of energy will occur. However, if the extraction pressure is too low, the flow in the low-pressure cylinder will change suddenly, which is harmful to the safe operation of the turbine. Therefore, the following analysis is based on the extraction from the fourth stage.

Fig. 6 shows that the increase in the extraction amount will cause a decrease in power generation and an increase in coal consumption, which is consistent with the analysis provided in Section 3.3. Clearly, however, because the steam consumption in a single LT-MED system is too small, the impact of the amount of steam extraction on the power generation and coal consumption of a single LT-MED system under different operating conditions is extremely limited. Therefore, to achieve a better understanding of the peak shaving performance of this

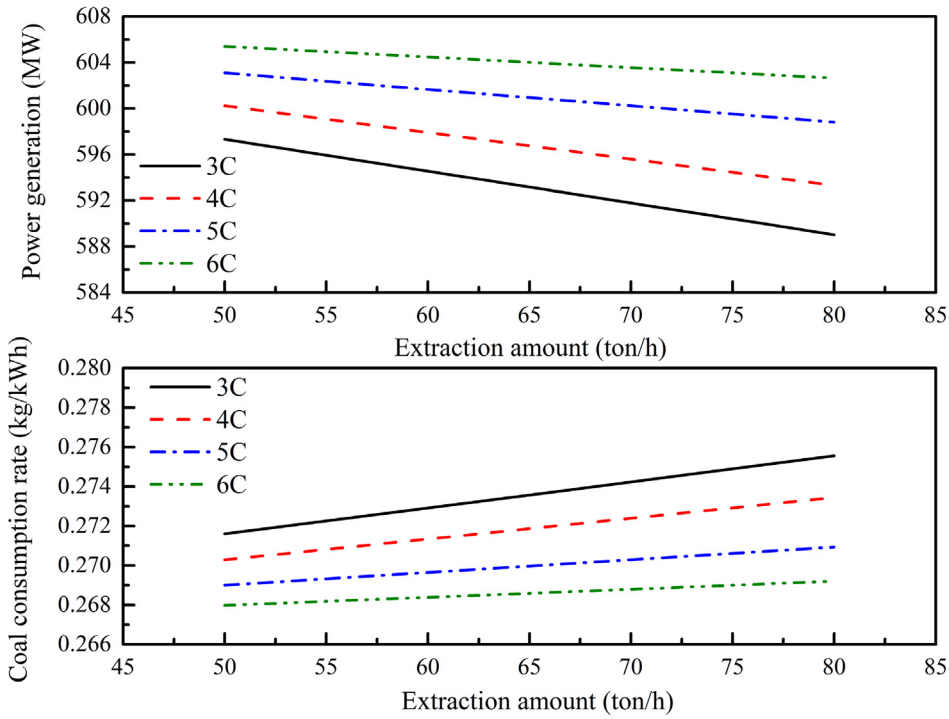

Fig. 3. Variations in power generation and coal consumption rate of the power generating unit based on the extraction point and amount.

coal-fired power plant, it is necessary to investigate the power generation under the maximum extraction amount of the unit and determine the corresponding water production performance if all of the extraction steam is used for seawater desalination.

3.5. Peak shaving performance of coal-fired power generating unit

When calculating the peak shaving capacity of the power plant, the core problem is finding the steam and condensation parameters in the thermodynamic cycles, which is limited by the maximum and minimum power generation of the unit.

The maximum output of the power plant corresponds to the BMCR condition, which is the condition assuring the safety and reliability of the boiler operation. The boiler is not allowed to operate beyond this condition. However, the minimum amount of main steam corresponds to the minimum steady combustion load of the boiler, and a 30% THA

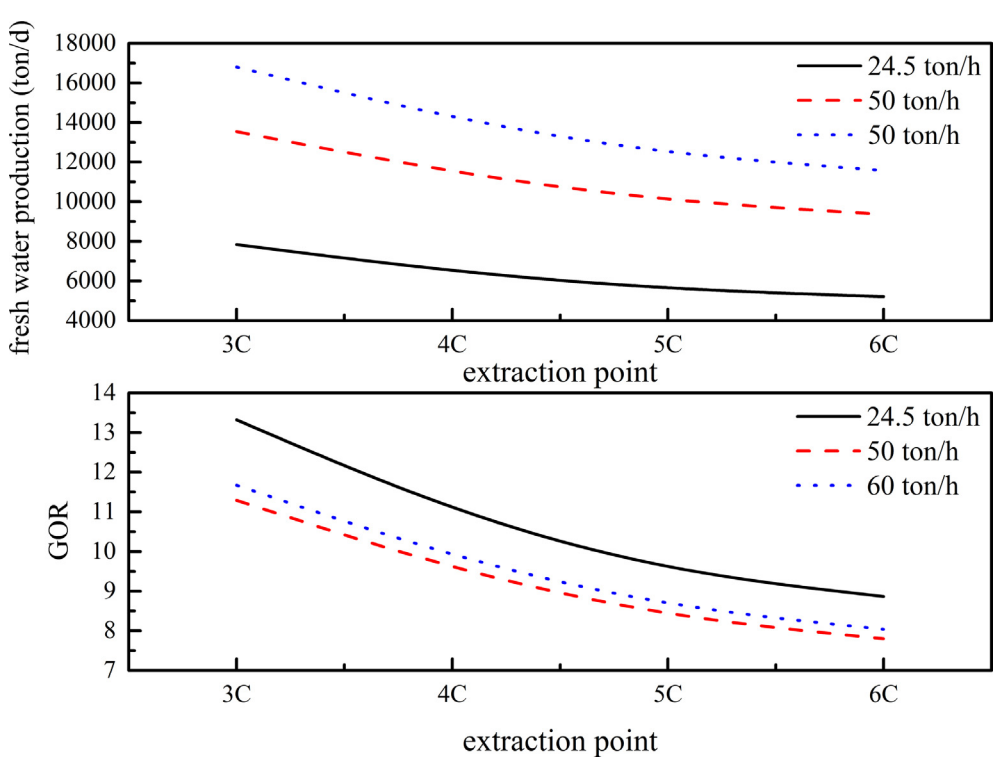

Fig. 4. Variations in fresh water production and GOR with extraction amount and extraction points.

Table 4
Initial conditions of the dynamic simulation.

Initial conditions	Value
Inlet seawater temperature, T_f, °C	25
Feed seawater temperature, T_{feed}, °C	41.8
Feed seawater temperature, T_{fin}, °C	48.8
Temperature of the first effect, °C	61.7
Temperature of the second effect, °C	58.4
Temperature of the third effect, °C	55.3
Temperature of the fourth effect, °C	52.3
Temperature of the fifth effect, °C	49.3
Temperature of the sixth effect, °C	46
Brine level of the first effect, m	0.8
Brine level of the second effect, m	1.07
Brine level of the third effect, m	1.19
Brine level of the fourth effect, m	1.09
Brine level of the fifth effect, m	0.7
Brine level of the sixth effect, m	0.2
Salinity of the first effect, g/kg	53.2
Salinity of the second effect, g/kg	52.6
Salinity of the third effect, g/kg	52
Salinity of the fourth effect, g/kg	51.5
Salinity of the fifth effect, g/kg	51.4
Salinity of the sixth effect, g/kg	51.5

operation condition is adopted in the present study. In addition, to ensure that there is a sufficient flow in the low-pressure cylinder, this flow varies with the different low-pressure cylinders applied, which is generally less than 15% of the designed maximum flow rate of the low-pressure cylinder, or approximately 5%–10% [31]. Under the above-mentioned limitations, the peak shaving capacity curve of the present objective power generating unit is as illustrated in Fig. 7.

In Fig. 7, with the changes in the amount of steam extracted from the turbine, AC and BD indicate the power generation when the boiler is under BMCR and 30% THA operating conditions, respectively. CD indicates the minimum exhaust steam flow from the low-pressure cylinder of the turbine, AB is the peak shaving capacity of a unit without a desalination system, and EF shows the peak shaving capacity of the unit with an extraction of 50 ton/h, which is the amount of steam consumption by the original desalination system. In addition, GH indicates the peak shaving capacity of the unit with an extraction of 75 ton/h, which is the steam consumption amount of an entire desalination plant containing the newly proposed desalination system. The area ABCD represents the peak shaving capacity of the present power generating unit.

Fig. 8 demonstrates the peak shaving capacity of the unit resulting from the BMCR and 30% THA curves shown in Fig. 7. By comparing Figs. 7 and 8, it can be seen that, with an increase in the extraction amount, the power generation of the unit is reduced but the peak shaving capacity is basically unchanged initially. The peak shaving capacity can reach up to 477 MW when the amount of steam extraction is less than 238 ton/h. A single desalination system has no effect on the peak shaving capacity of the power generation unit, which is consistent with the analysis described in Section 3.4. When the amount of

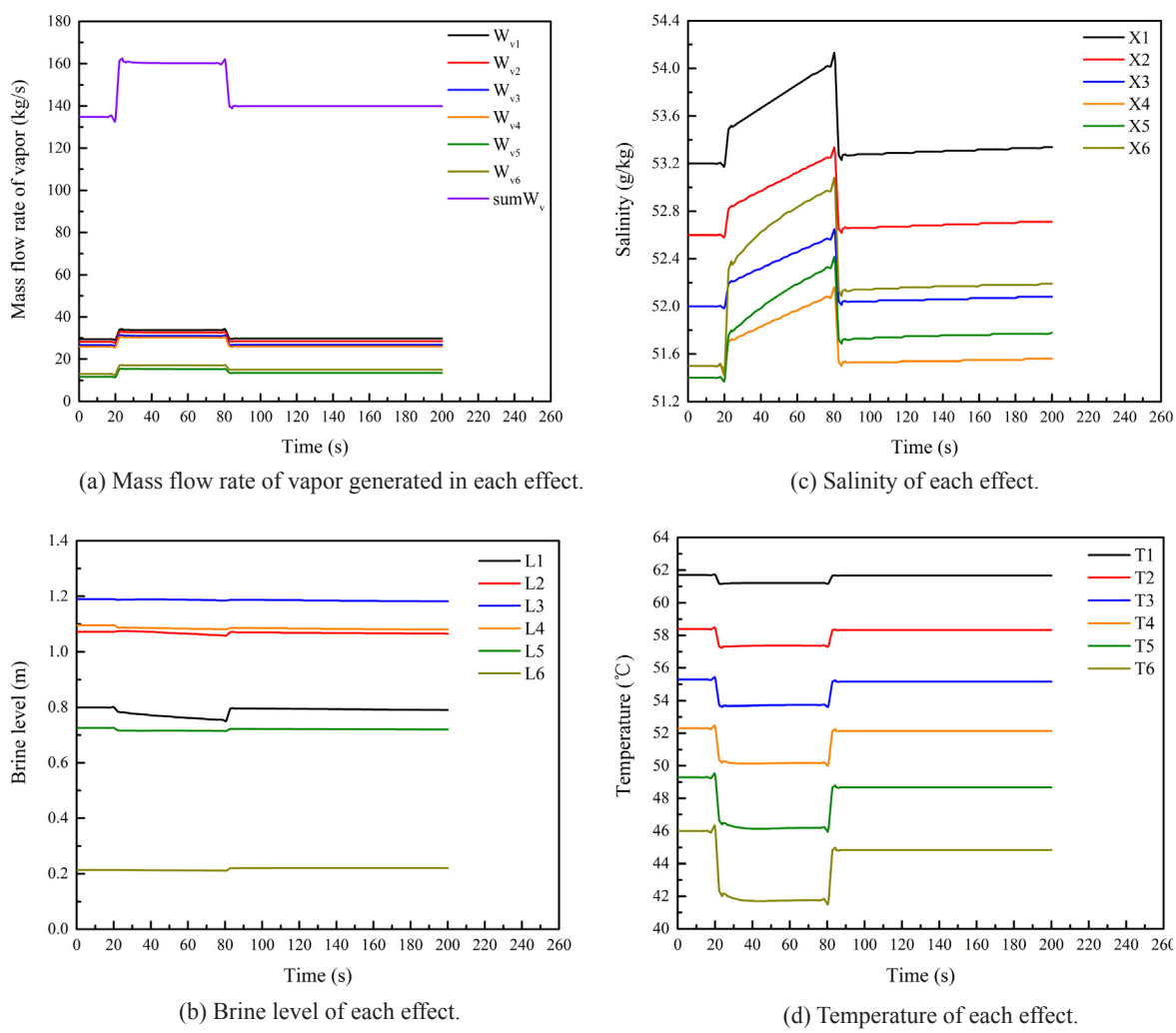

(a) Mass flow rate of vapor generated in each effect.

(c) Salinity of each effect.

(b) Brine level of each effect.

(d) Temperature of each effect.

Fig. 5. Dynamic response of LT-MED system to improved steam extraction from steam turbine.

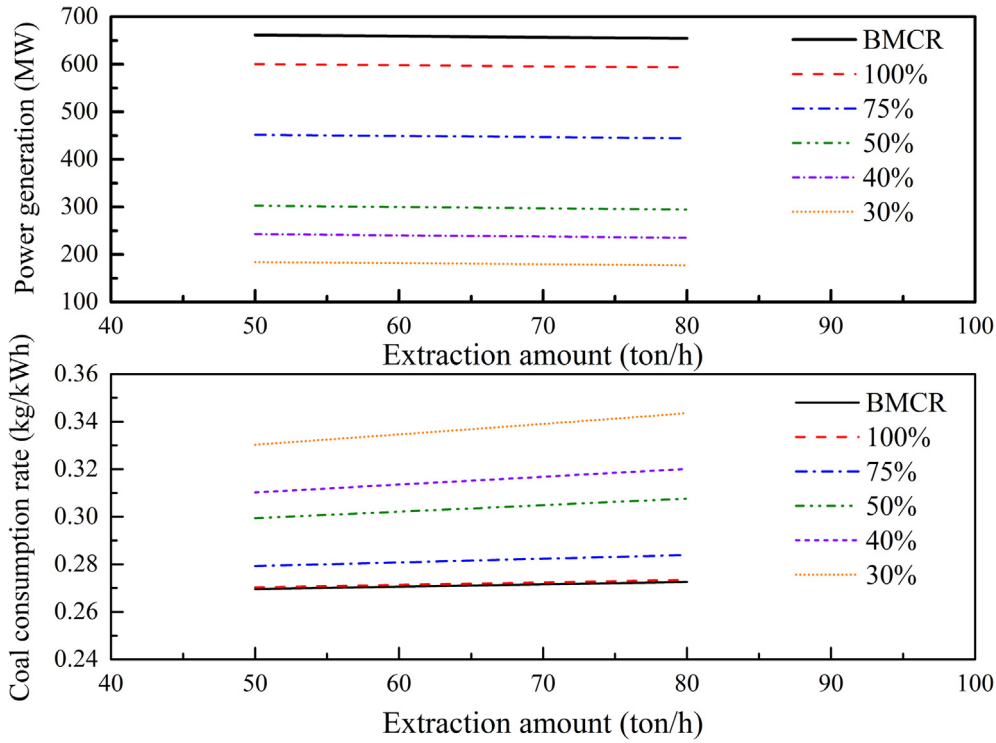

Fig. 6. Variations in power generation and coal consumption rate of a power plant under different operating conditions and extraction amounts.

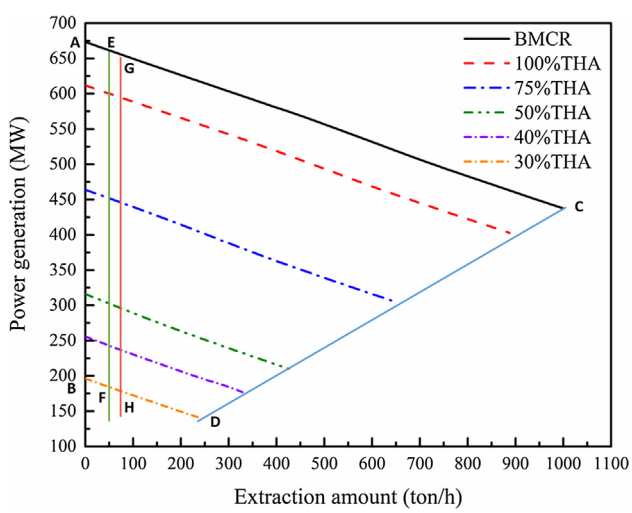

Fig. 7. Peak shaving capacity curve of the power generating unit.

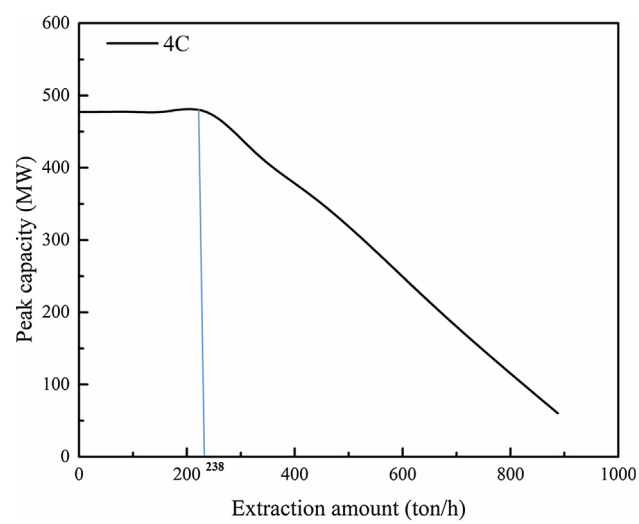

Fig. 8. Peak shaving capacity of the power generating unit when extracting steam from the fourth stage of the steam turbine.

extraction is sufficiently large to make the exhaust steam from the low-pressure turbine reach the minimum allowable value, the peak shaving capacity of the unit sharply decreases. However, for the present power and water co-generation system, a portion of the extracted steam can be used to drive the desalination section. For a frequent peak shaving off-shore power generating unit, it can be considered that excess extraction steam can be used to provide more desalination systems.

Consider a situation in which extraction is used for seawater desalination. Points A and B in Fig. 7 are cases with no extraction, and no fresh water production occurs at these points in time. Points E and F correspond to the original desalination system when the extraction amount is 50 ton/h, and the fresh water production is 10,000 ton/d. Points G and H correspond to the entire desalination system when the amount of extraction is 75 ton/h, and the fresh water production is 22,000 ton/d. Points C and D are the maximum extraction amounts of the BMCR and 30% THA conditions, respectively, which are used for N new LT-MED systems in the following calculation. When a new LT-MED system is operated under the design conditions, the extraction amount at point C can afford approximately 19 LT-MED systems, and point D, approximately 3.75 LT-MED systems.

Because points E, F, G, and H involve the original desalination system, and owing to a lack of operating data, the corresponding GOR and water production cost cannot be calculated. Therefore, Table 5 lists

Table 5
Maximum GOR and water production cost of a single LT-MED system.

	GOR	Water production cost ($/m^3)
Point C	9.822	2.152
Point D	10.12	2.123

only the maximum GOR and water production cost of a single LT-MED system corresponding to points C and D.

The extraction pressure at point D is slightly lower than that at point C. The enthalpy of extraction steam at point D is higher than that at point C. Owing to the need for spray desuperheating, more steam enters the first effect, thereby increasing the GOR and reducing the water production cost. This also shows that a proper reduction of the extraction pressure is conducive to reducing the water production costs.

4. Conclusions

The widely-used LT-MED seawater desalination system was selected to assist a 600 MW coal-fired power generating unit in adjusting the output load. This not only helps reduce the difficulty of engineering but also benefits the promotion of renewable energy power generation in the grid system. The effects of the extraction points and extraction amount on the unit power generation and water production were studied. Depending on the different extraction amounts, the peak shaving capacity curve was obtained. Thermodynamic and dynamic analyses were also conducted to analyze the response of an LT-MED system to the output power variation. The following conclusions can be drawn.

(1) As the amount of steam extraction increases, the power generation decreases and the coal consumption increases. With the same extraction amount, as the extraction point moves backward, the power generation increases, the coal consumption decreases, and the fresh water production is reduced.
(2) With an increase in the extraction amount, the power generation of the unit is reduced although the peak shaving capacity is basically unchanged initially. The peak shaving capacity can reach up to 477 MW when the amount of steam extraction is less than 238 ton/h. When the extraction amount is sufficiently large to make the exhaust steam from the low-pressure turbine reach the minimum allowable value, the peak shaving capacity of the unit sharply decreases.
(3) To couple the step reduction of the output power load of the power generating unit, the sudden increase of steam into the first effect of the LT-MED system leads to an increase in the secondary vapor and salinity in each effect. Simultaneously, a decrease in the temperature of each effect is observed. The change of the above items caused by the decrease in the steam pressure is opposite.
(4) The steam consumption in a single LT-MED system is too small to have a significant impact on the power generation or coal consumption under the different operating conditions. The maximum extraction amount of the unit under the BMCR can afford approximately 19 LT-MED systems. The maximum extraction amount under a 30% THA can afford approximately 3.75 LT-MED systems. A proper reduction of the extraction pressure is conducive to reducing the water production costs.

Acknowledgement

The financial supports for this study from the National Natural Science Foundation of China (No. 51676069, 51821004) and the national “973 Program” of China (No. 2015CB251503) are gratefully acknowledged.

References

[1] Wind power development “Thirteen-Five” plan. National energy administration of China; 2016 [in Chinese].
[2] Electric power development “Thirteen-Five” plan. National energy administration of China; 2017 [in Chinese].
[3] Electricity production statistics of 2017. National bureau of statistics of China; 2018 [in Chinese].
[4] Peng Z, Chen Q, Yang Y, Xia Q, Kang C. Electricity markets evolution with the changing generation mix: An empirical analysis based on China 2050 high renewable energy penetration roadmap ☆. Appl Energy 2017;185:56–67.
[5] Jung Vanli A, Kwon SoonDuck. Wind energy potential assessment considering the uncertainties due to limited data. Appl Energy 2013;102:1492–503.
[6] Zhou S, Wang Y, Zhou Y, Clarke LE, Edmonds JA. Roles of wind and solar energy in China’s power sector: Implications of intermittency constraints. Appl Energy 2018;213:22–30.
[7] González-Aparicio I, Zucker A. Impact of wind power uncertainty forecasting on the market integration of wind energy in Spain. Appl Energy 2015;159:334–49.
[8] Gu Y, Xu J, Chen D, Wang Z, Li Q. Overall review of peak shaving for coal-fired power units in China. Renew Sustain Energy Rev 2016;54:723–31.
[9] Shen Li, Xu Shude, Guan Jian, Lu Hongyue, Qiu Lichun. Effects of deep participation in peak regulation on the coal-fired boiler of a supercritical high-capcacity thermal power plant. Power Equipment 2016;30:21–3. [in Chinese].
[10] Wu Ruikang, Hua Min, Qin Pan, Bao Jinsong, Lou Kewei, Ding Yangjun, Fan Yinlong. Influence of deep peak load regulation of coal-fired units on turbine equipment. Therm Power Generation 2018;5:89–94. [in Chinese].
[11] Divya KC, Østergaard J. Battery energy storage technology for power systems—An overview. Electr Power SystRes 2008;79:511–20.
[12] Garbrecht O, Bieber M, Kneer R. Increasing fossil power plant flexibility by integrating molten-salt thermal storage. Energy 2017;118:876–83.
[13] Aneke M, Wang M. Energy storage technologies and real life applications – A state of the art review. Appl Energy 2016;179:350–77.
[14] He W, Wang J. Feasibility study of energy storage by concentrating/desalinating water: concentrated water energy storage. Appl Energy 2017;185:872–84.
[15] Frank H, Rahav E, Bar-Zeev E. Short-term effects of SWRO desalination brine on benthic heterotrophic microbial communities. Desalination 2017;417:52–9.
[16] Ghaffour N, Bundschuh J, Mahmoudi H, Goosen MFA. Renewable energy-driven desalination technologies: A comprehensive review on challenges and potential applications of integrated systems. Desalination 2015;356:94–114.
[17] Wunder F, Enders S, Semiat R. Numerical simulation of heat transfer in a horizontal falling film evaporator of multiple-effect distillation. Desalination 2017;401:206–29.
[18] Qi CH, Feng HJ, Lv QC, Xing YL, Nan L. Performance study of a pilot-scale low-temperature multi-effect desalination plant. Appl Energy 2014;135:415–22.
[19] Zhang F, Xu S, Feng D, Chen S, Du R, Su C, Shen B. A low-temperature multi-effect desalination system powered by the cooling water of a diesel engine. Desalination 2017;404:112–20.
[20] Talebbeydokhti P, Cinocca A, Cipollone R, Morico B. Analysis and optimization of LT-MED system powered by an innovative CSPplant. Desalination 2017;413:223–33.
[21] Bundschuh J, Ghaffour N, Mahmoudi H, Goosen M, Mushtaq S, Hoinkis J. Low-cost low-enthalpy geothermal heat for freshwater production: Innovative applications using thermal desalination processes. Renew Sustain Energy Rev 2015;43:196–206.
[22] Al-Othman A, Darwish NN, Qasim M, Tawalbeh M, Darwish NA, Hilal N. Nuclear desalination: A state-of-the-art review. Desalination 2019;457:39–61.
[23] Mahbub F, Hawlader MNA, Mujumdar AS. Combined water and power plant (CWPP) — a novel desalination technology. Desalin Water Treat 2009;5:172–7.
[24] Xue Y, Du X, Ge Z, Yang L. Study on multi-effect distillation of seawater with low-grade heat utilization of thermal power generating unit. Appl Therm Eng 2018;141:589–99.
[25] El-Dessouky HT, Ettouney HM, Mandani F. Performance of parallel feed multiple effect evaporation system for seawater desalination. Appl Therm Eng 2000;20:1679–706.
[26] Mazini MT, Yazdizadeh A, Ramezani MH. Dynamic modeling of multi-effect desalination with thermal vapor compressor plant. Desalination 2014;353:98–108.
[27] El-Dessouky HT, Ettouney HM. Fundamentals of salt water desalination. Elsevier Science B.V. ; 2002 .
[28] Nayar KG, Sharqawy MH, Banchik LD, John HLV. Thermophysical properties of seawater: A review and new correlations that include pressure dependence. Desalination 2016;390:1–24.
[29] Xu C, Bai P, Xin T, Hu Y, Xu G, Yang Y. A novel solar energy integrated low-rank coal fired power generation using coal pre-drying and an absorption heat pump. ApplEnergy 2017;200:170–9.
[30] Zhao S, Ge Z, He J, Wang C, Yang Y, Li P. A novel mechanism for exhaust steam waste heat recovery in combined heat and power unit. Appl Energy 2017;204:596–606.
[31] Liu ZZ. Combined heat and power. Beijing: China Electric Power Press; 2006. [in Chinese].